Water Body Detection and Delineation with Landsat TM Data

Paul Shane Frazier and Kenneth John Page

Abstract

The aim of this project was to determine the accuracy of using simple digital image processing techniques to map riverine water bodies with Landsat 5 TM data. This paper quantifies the classification accuracy of single band density slicing of Landsat 5 TM data to delineate water bodies on riverine floodplains. The results of these analyses are then compared to a 6-band maximum likelihood classification over the same area. The water boundaries delineated by each of these digital classification procedures were compared to water boundaries delineated from colour aerial photography acquired on the same day as the TM data. These comparisons show that Landsat TM data can be used to map water bodies accurately. Density slicing of the single mid-infrared band 5 proved as successful as multispectral classification achieving an overall accuracy of 96.9%, a producer's accuracy for water bodies of 81.7% and a user's accuracy for water bodies of 64.5%.

Introduction

Accurate information on the extent of water bodies is important for flood prediction, monitoring, and relief (Smith, 1997; Tholey *et al.*, 1997; Baumann, 1999); production of wetland inventories (Bennett, 1987; Johnston and Barson, 1993; Blackman *et al.*, 1995; Shaikh *et al.*, 1998; Phinn *et al.*, 1999); and the evaluation of water resources (Morse *et al.*, 1990; Manavalan *et al.*, 1993). Often this information is difficult to produce using traditional survey techniques because water bodies can be fast moving as in floods, tides, and storm surges or may be inaccessible. Remotely sensed data provide a means of delineating water boundaries over a large area at a given point in time. To capture fast moving hydrological features, the data need to be either of a high temporal resolution or in a substantial archive to cover a range of hydrological conditions. Landsat MSS and TM provide high spatial resolution data at 16-day intervals over a long archival history, exceeding 25 years in most locations. The long archive period and repetitive capture make the data useful for mapping water bodies at a regional scale over a range of hydrological conditions.

Since Landsat data became available in 1972, they have been used to map water extent. Smith (1997) cites several early studies where Landsat MSS data, in particular Band 7, were used to distinguish water bodies from surrounding dry soil or vegetation. Comparison with aerial photography gave error estimates of less than 5 percent.

Bennett (1987) used density slicing of Landsat MSS band 7 to map water bodies to the west of Griffith, New South Wales, Australia (NSW). He compared the area of MSS-derived water bodies with that derived from digitized aerial photography and found that the MSS data underestimated the area of water by around 40 percent.

Johnston and Barson (1993) evaluated the usefulness of Landsat TM imagery for mapping lake/pond wetland extent in western Victoria and riverine wetland extent in central Victoria. The satellite information was compared to manually mapped ground truth. They found that simple density slicing of the TM5 (mid-infrared) successfully detected the lake/pond wetland areas achieving a classification accuracy of 95 percent but failed to map the riverine wetlands adequately. The failure of the technique with riverine wetlands was attributed to the narrow width of the oxbow lakes and a poor timing of data selection.

Many other studies have reported the successful use of density slicing of Landsat TM or MSS data to delineate water bodies; however, no quantitative accuracy assessments were conducted. Manavalan *et al.* (1993) used Landsat TM band 4 to map the extent of the Bhadra Reservoir, India. Overton (1997) used density slicing of Landsat TM band 5 and a high flood spatial mask to map water bodies on the Murray River between Blanchetown and Wentworth, South Australia. Shaikh *et al.* (1997) timed the acquisition of Landsat MSS band 7 to coincide with selected significant hydrological events to determine wetland inundation for the Cumbung Swamp, NSW, Australia. Baumann (1999) used band 4 of Landsat TM to map flood extent on the Mississippi River but experienced problems separating water from certain urban features without the inclusion of an additional band.

Other studies have successfully used both supervised and unsupervised multispectral classification of optical remote sensing data to delineate water boundaries (Manavalan *et al.*, 1993; Lee and Lunetta, 1995; Blackman *et al.*, 1995; Kingsford *et al.*, 1997; Brady *et al.*, 1999). Kingsford *et al.* (1997) used supervised maximum-likelihood classification of Landsat MSS data to map wetlands over a part of the Murray-Darling Basin. Checking of 200 random water bodies with aerial photography gave an accuracy of 90 percent. They then extended the project to the entire basin using 59 images and an unsupervised classification procedure.

Both single-band density slicing and multispectral classification (supervised and unsupervised) have been used to map water boundaries. Researchers typically have relied upon visual comparisons between the classification and the raw data to estimate accuracy. Few studies have used a formal accuracy assessment procedure. Where statistical accuracy assessment procedures have been implemented, they have either compared the area or number of wetlands identified by ground truth with that determined from the satellite image, or they

School of Science and Technology, Charles Sturt University, Locked Bag 588, Wagga Wagga, NSW 2678, Australia (pfrazier@csu.edu.au).

Photogrammetric Engineering & Remote Sensing
Vol. 66, No. 12, December 2000, pp. 1461–1467.

0099-1112/00/6612–1461$3.00/0

have used a random sampling procedure to check the classification accuracy. These methods of accuracy assessment do allow the production of a formal estimate of the error in the classification but provide no information on where the classification performed badly or where it performed well. To select useful image bands and determine the optimum classification procedure for water body delineation, a comparison of the different techniques using a quantitative spatial accuracy assessment is needed.

This project set out to determine the classification accuracy of density slicing and multispectral image classification of Landsat 5 TM data to map the water bodies of the Murrumbidgee River and floodplain near Wagga Wagga, Australia (Figure 1). Landsat TM data were classified using single-band density slicing and multispectral maximum-likelihood classification. These classified data were then compared to high resolution aerial photography to determine how well the Landsat data could be used to detect and delineate water bodies.

Specifically this project set out to

- Quantify the accuracy of simple digital techniques for the detection and delineation of riverine floodplain water bodies using Landsat TM data,
- Recommend a suitable technique for mapping riverine floodplain water bodies, and
- Determine the best band or set of bands required for water boundary mapping.

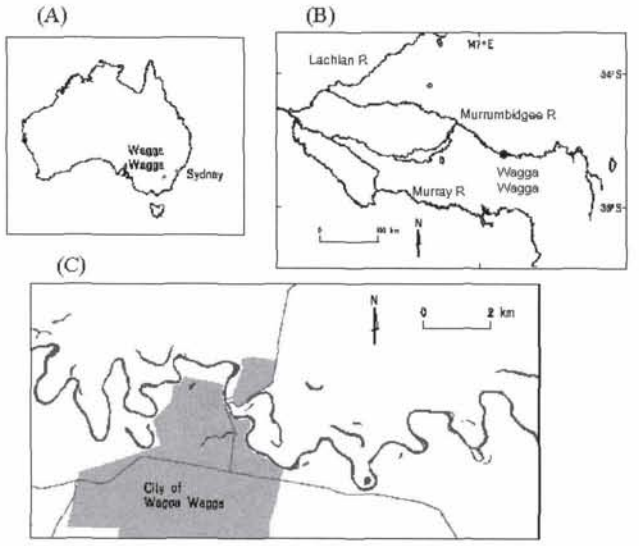

Figure 1. The location of (A) the City of Wagga Wagga in Australia, (B) the Murrumbidgee River within the southern Murray-Darling Basin, and (C) the study reach near Wagga Wagga.

The Study Area

The study examines the channel and floodplain of the Murrumbidgee River near the city of Wagga Wagga, in a reach extending 15.3 km by 5.6 km (Figure 1). The Murrumbidgee River forms a part of the Murray-Darling basin and drains an area of approximately 82 000 km^2 (Olive *et al.*, 1994). In the study reach it is a large meandering river with an average bankfull channel width of 80 m, a mean depth of 6 m, a sinuosity of 2.3, and has a predominantly suspended load (Page, 1988).

The river floodplain is 1 to 2 km wide (Olive *et al.*, 1994) and consists of 6 to 7 m of mud and sand overlying basal gravels. There are several types of natural water bodies on the floodplain, including lagoons (meander cut-offs or oxbow lakes), interscroll swales, and backswamp depressions (Table 1). The lagoons are large water bodies, often greater than 6 hectares in size, with a width similar to that of the active channel and with considerable variability in turbidity and depth. The interscroll swales are smaller features, often less than 10 m wide, that contain water for variable but usually short periods after floods or heavy rain. Backswamps are shallower depressions that hold water for an extended period. They are not common features in the study reach. Several artificial dams are also found in this area. The largest of these is the effluent storage pond for the Wagga Wagga sewerage works (Figure 2).

Figure 3 shows the discharge hydrograph for the Wagga Wagga gauging station from July 1990 to November 1990. At the time of data capture (26 October 1990), the floodplain retained water from a flood event that occurred on 08 July 1990. This event had a maximum discharge of 63,000 Ml/d, sufficient to over top the river bank in this reach and fill many of the floodplain wetlands (Page, 1988). Flood events of this size can carry very turbid water with a sediment concentration of over 400 mg/l (Olive and Olley, 1997). On the day of data capture the river at Wagga Wagga had a flow of 24,000 Ml/d (Pinneena, 1998) with a turbidity of 90 mg/l (Southern Riverina County Council, water quality archive, 26 October 1990).

Methods

In order to assess the accuracy of using Landsat TM data to accurately locate and delineate water bodies, classified Landsat TM data were compared with manually mapped aerial photography of the same area. Luckily for this study, both the Landsat TM data and the aerial photography were captured on the same date (26 October 1990), thus ensuring identical hydrological conditions.

Materials

The color aerial photography was acquired by the NSW Central

TABLE 1. CLASSES AND DESCRIPTIONS OF DIGITIZED WATER BODIES.

Polygon label	Description	Dimensions	Vegetation
River	Active channel of Murrumbidgee River (single linear feature)	Water surface width 50 to 100 m Max depth 8 to 10 m	Marginal trees < 5% crown cover
Lagoon	Abandoned reaches of Murrumbidgee channel (seven features)	Water surface width 50 to 100 m Max depth 1 to 4 m Area 6 to 18 ha	Marginal trees < 5% crown cover
Small Pool	Smaller water bodies on floodplain (closed depression in swales and backswamps) (105 features)	Variable shape Max depth 0.2 to 2 m Area 0.005 to 3.2 ha	Marginal trees < 10% crown cover
Dam	Artificial water bodies Sewerage ponds, one gravel pit (3 features)	Variable shape Max depth 1 to 8 m Area 2.8 to 14.5 ha	Nil

Mapping Authority at a nominal scale of 1:25,000. For this project, prints 142–148 of run 3 were used. A subset of the Landsat TM scene (Path/Row 92/84, level 4 processing), covering the same area as the selected aerial photography, was excised from the original data. This procedure resulted in the creation of an image of 510 pixel by 187 lines with bands 1,2,3,4,5, and 7 (Figure 1). ERMapper software Version 5.7 was used for all image processing, polygon digitizing, and polygon manipulation.

Aerial photograph interpretation

The aerial photographs were scanned at 300 DPI using a Microtek ScanMaker 9600XL A3 flatbed scanner. The resulting images had an approximate ground pixel size of 2.1 m. The digital images were then registered to the TM imagery using eight ground control points (GCPs) per photograph. The GCPs were selected as close as possible to the margins of the water bodies on each photograph in order to maximize the likelihood of a good match to the TM data.

The first attempt at registration gave an average root-mean-square (RMS) error of 10 pixels (21 m). The images were then warped using a linear geometric transformation, nearest-neighborhood intensity interpolation, and a pixel resampling size of 3 m. Examination of the fit between the photographs and the TM data indicated that there were significant registration errors. Each photograph was then re-registered using an additional seven GCPs on the margins of the water bodies, achieving an average RMS error of ±3 pixels (9 m). This time overlaying the photograph onto the TM image indicated a good fit.

All water bodies greater than 625 m^2 (1mm by 1mm) in size were then highlighted directly on the hardcopy prints of photographs 143, 145, and 147 using magnified stereoscopic examination. On the photographs, water bodies appear as uniform regions of dark green to bright khaki brown in the low lying channels and depressions. Each water body was then digitized directly onto the scanned, registered aerial photograph using the ERMapper regions tool. The polygons were then labeled as River, Lagoon, Small Pool, or Dam (Table 1, Figure 2). The polygons were then converted into a five-class raster image for comparison with the Landsat TM classification results.

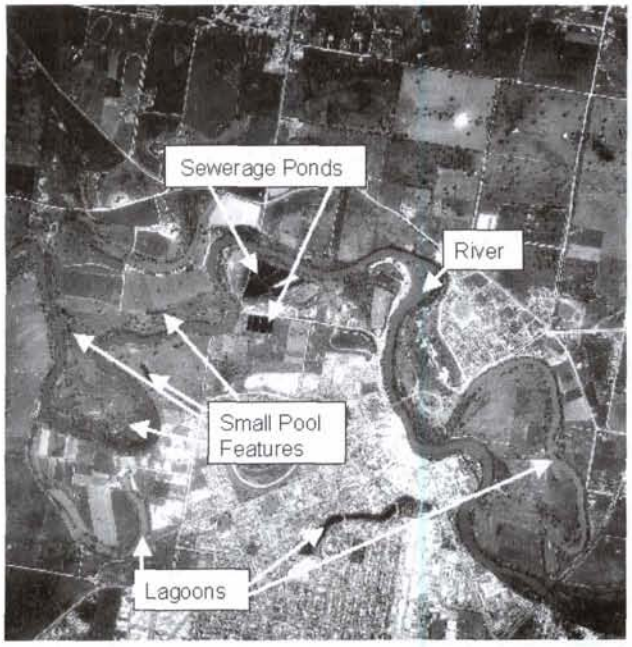

Figure 2. Aerial photograph of the Wagga Wagga region (print 146) showing water body types.

Landsat Image Classification

Single-band density slicing and the multispectral maximum-likelihood algorithm were used to classify the satellite data. The density slicing attempted to quantify the accuracy of a simple technique using a single band to map water bodies. The more advanced multispectral classification was completed to give a benchmark result using all reflective bands for comparison with the density slicing results.

Interrogation of the data was carried out through the selection of 12 training areas over various water bodies. These training areas were selected from a range of river, lagoon, and dam sites to account for the full range in water reflectance resulting from different water depths and turbidities. Figure 2 shows that even within the lagoon class of water bodies there is consider-

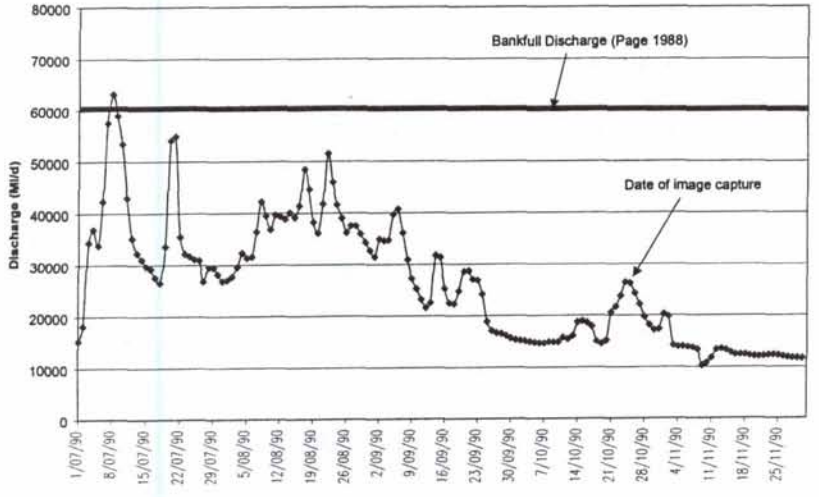

Figure 3. Discharge hydrograph for the Murrumbidgee River at Wagga Wagga July to November 1990.

able variation in water brightness.

The statistics of each training site were analyzed to determine which band or bands best discriminated water bodies from the surrounding landscape (Table 2). There was considerable variation in the mean water values between training sites in each of the visible bands. Band 4 shows a reduced variation between mean values with bands 5 and 7 showing even less variation.

A simple density slice classification of each band was used to determine which bands were most useful for water boundary discrimination. The minimum and maximum value of water from the combined training site values (Table 3) were used to create the boundaries of the density slicing procedure.

The maximum-likelihood classification was completed using all 12 "water" training areas (Table 2). Classified pixels that were less than 2 percent typical of the training statistic were eliminated from the classification. The resulting 12 water classes were then combined into one super "water" class.

The density slice classification of each band and the maximum-likelihood classification were then compared with the raster ground-truth data on a per pixel basis.

Results and Discussion

Density Slicing

Figure 4 shows a section of the density slicing results for each TM band. Clearly, the classifications of the three visible bands substantially overestimate the area of water on the image. There is considerable spectral overlap between the brightness values found in the water bodies and those in the surrounding urban and rural landscape (Figure 5).

The infrared band classifications all give a much better representation of the water bodies than do the visible bands. Band 4 is able to identify most of the major water bodies, but there is still some confusion with the urban area, hill shadows, and poor pasture paddocks. The density slicing of band 7 also gives a reasonable representation of the water boundaries but includes some very lush crop paddocks that may be undergoing irrigation.

Density slicing of band 5 gave the best visual approximation of the ground-truth image without including other land-cover types. Based on aerial photograph interpretation and local knowledge, the only major error of commission appears to be very moist or waterlogged soil areas on the flood plain.

The overall classification accuracy along with producer's and user's accuracies (Jensen, 1996) for the water class from each of the six bands are presented in Table 4. As expected from the visual interpretation, the visible bands perform badly when it comes to differentiating water bodies from other land-cover types. The overall classification accuracies for each of these bands were all below 8 percent. Because the number of pixels classified as water is very high for the visible bands, the producer's accuracies were all very high, being above 96 percent in each case. However, these results are offset by the very poor user's accuracies, of less than 5 percent.

The three infrared bands all perform significantly better than the visible bands, achieving high overall accuracies and greatly increased user's accuracies. The result from band 5 achieved the best) combination of accuracy results with the highest overall accuracy (96.9 percent), a producer's accuracy of 81.7 percent, and the highest user's accuracy at 64.5 percent (Table 4).

TABLE 2. MEAN WATER BODY TRAINING SITE VALUES OF EACH LANDSAT TM BAND.

	Mean Pixel Value					
Training Site	Band 1	Band 2	Band 3	Band 4	Band 5	Band 7
Lagoon 1	84.31	41.50	53.58	26.12	12.29	2.91
Lagoon 2	70.42	29.96	33.27	25.04	13.69	3.39
Lagoon 3	95.76	50.56	65.84	33.84	11.80	3.26
Lagoon 4	73.84	31.63	36.21	18.21	15.37	3.94
Lagoon 5	83.32	40.73	48.23	30.41	16.91	3.68
Lagoon 6	71.87	29.48	34.22	24.35	17.96	4.38
River 1	71.68	29.59	32.50	22.18	15.14	4.27
River 2	71.00	29.50	32.30	16.40	12.50	2.22
River 3	70.28	28.65	31.30	16.56	9.85	2.37
River 4	67.68	27.21	28.11	22.00	13.04	3.82
Dam 1	61.60	19.95	16.19	20.57	15.15	4.30
Dam 2	59.75	19.00	16.83	19.75	15.25	4.55
Standard Deviation	10.03	8.94	14.24	5.34	2.30	0.78

TABLE 3. MAXIMUM AND MINIMUM VALUES FOR ALL WATER BODY TRAINING AREAS.

Band	Minimum Water Value	Maximum Water Value
1	57	100
2	23	55
3	21	71
4	14	66
5	2	47
7	1	13

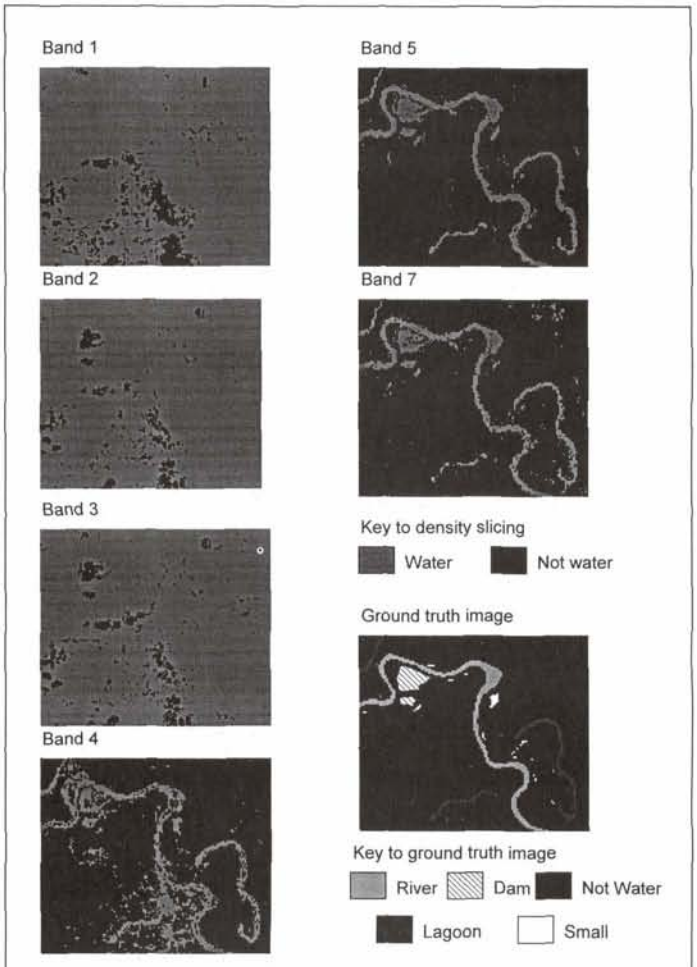

Figure 4. Results of density slicing each Landsat TM band.

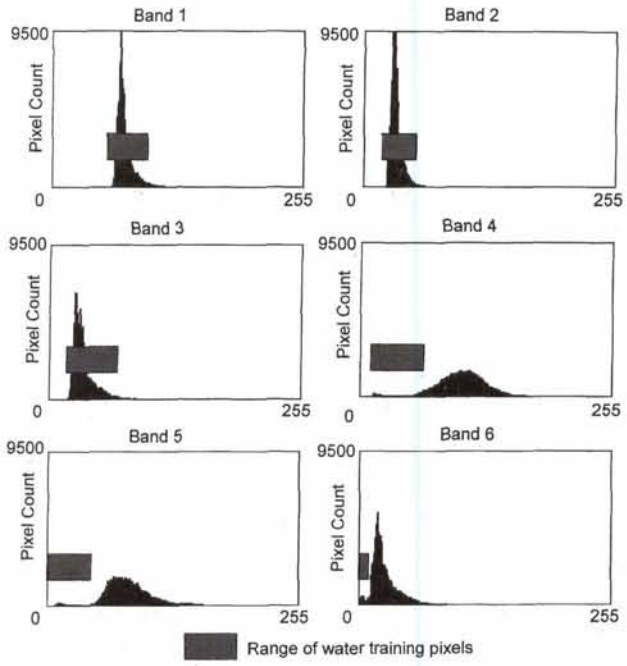

Figure 5. Individual band histograms and water training pixel ranges.

TABLE 4. RESULTS OF LANDSAT TM CLASSIFICATION ACCURACY ASSESSMENT.

Band	Overall Classification Accuracy (%)	Water Class Producer's Accuracy (%)	Water Class User's Accuracy (%)
1	7.7	99.6	5.0
2	6.4	96.7	4.8
3	8.0	96.5	4.9
4	93.6	77.1	42.6
5	96.9	81.7	64.5
7	94.4	74.4	45.4

A more detailed analysis of the results from the band 5 classification is presented in Table 5. This table shows that the classification is good at mapping areas that are not water, a result that is not suprising given that the ground-truth mapping indicates that the area consists of 95.1 percent non-water land cover. However, it also indicates that the classification did not contain major errors of commission.

Of more interest is the ability of the classification to detect water bodies. Clearly, the classification does a reasonable job of detecting and delineating the larger water bodies (River, Lagoon, and Dam classes) with results above 80 percent. The smaller water bodies are not as well represented, with an accuracy of only 48.2 percent. Many of these smaller water bodies were often less than a single pixel in size, and most of them were less than a pixel in width. The size of these water bodies ensured that the classification was trying to map a mixed pixel. Even the strong absorbance characteristics of water on infrared electromagnetic radiation did not prevent the mixed pixel being mapped as a non-water area.

The reason for the failure of the density slicing of the visible bands to accurately classify the water boundaries is shown in Figure 5. The range of the density slicing determined from the water training areas covers almost the entire range of data in each of the visible bands. Therefore, the resulting classification covers almost the entire image, as indicated on Figure 4. Each of the visible bands displays a uni-modal histogram with no indication of a separate group of data for water pixels.

The infrared bands all display a bi-modal histogram with a darker mode consisting mostly of water pixels. The density slice ranges for band 5 and band 7 start at near zero, meaning that water pixels are the darkest in the image. The range for each of these bands slightly overlaps with the largest mode in the histogram. The density slice range of 14 to 66 for band 4 does not account for all of the pixels in the smaller darker mode and significantly overlaps with the darker edge of the main pixel mode.

Maximum-Likelihood Classification

The supervised maximum-likelihood classification produced the best overall accuracy of 97.4 percent, a producer's accuracy of 59.6 percent, and a user's accuracy of 81.4 percent. The error breakdown, presented in Table 6, indicates that the maximum-likelihood classification, like the band 5 density slice, was very good at accurately mapping areas of not water.

The supervised classification proved to be more sensitive than the density slicing method for detecting water bodies and produced fewer errors of commission. However, this sensitivity excluded more atypical water pixels, creating a larger error of omission (ie. lower producer's accuracy). For each of the four water body types the maximum likelihood classification performed significantly worse than the band 5 density slice. The percentage accuracy for the Small Pool, Dam, River, and Lagoon water bodies is 21.4 percent, 56.3 percent, 66.3 percent, and 57.5 percent, respectively, for the maximum-likelihood classification as opposed to 48.2 percent, 85.0 percent, 86.2 percent, and 81.2 percent for the band 5 density slice (Table 6 and Table 5, respectively).

Figure 6 illustrates the differences between the results of the band 5 density slice and the maximum-likelihood classification. The density slice result gives a less speckled representation of the water bodies but suffers from inclusion of some pixels that clearly are not water bodies but are dark enough to fall into the same brightness range.

Conversely, the supervised maximum-likelihood classifi-

TABLE 5. ERROR MATRIX FROM BAND 5 CLASSIFICATION.

Band 5 Error Matrix		Classification Data: Water	Not Water	Total	Percentage Correct
Reference	Small Pool	212	228	440	48.2%
	Dam	164	29	193	85.0%
	River	2626	419	3045	86.2%
	Lagoon	777	173	950	81.8%
	Not Water	2079	88663	90742	97.7%
	Total	5858	89512	95370	—
Percentage Correct		64.5%	99.1%	—	96.9%

TABLE 6. SUPERVISED MAXIMUM LIKELIHOOD CLASSIFICATION ERROR MATRIX.

Maximum-Likelihood Classification Error Matrix		Classification Data			
		Water	Not Water	Total	Percentage Correct
Reference	Small Pool	94	346	440	21.4%
	Dam	535	415	950	56.3%
	River	2018	1027	3045	66.3%
	Lagoon	111	82	193	57.5%
	Not Water	629	90113	90742	99.3%
	Total	3390	91980	95370	—
Percentage Correct		81.4%	98.0%	—	97.4%

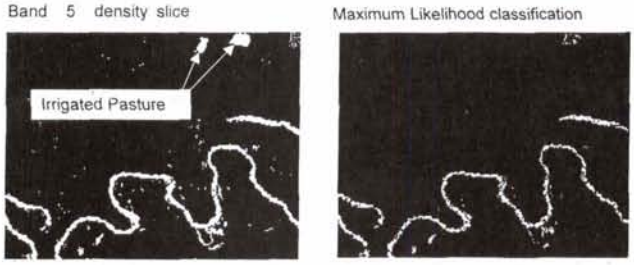

Figure 6. Water bodies identified by the band 5 density slice and the maximum-likelihood classification methods.

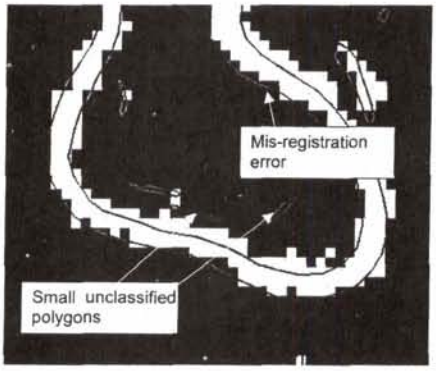

Figure 7. The affect of misregistration and small polygons on the accuracy of Landsat TM classification.

cation presents a more speckled representation of the water bodies. The greater sensitivity of this classifier appears to have excluded more pixels that are atypical of the main training data but were mapped as water on the ground truth.

The Effects of Registration Errors

In any situation where long slender polygons are being matched to an image, registration errors or distortions in either the image or the polygons can contribute to the overall error count. A closer viewing of the band 5 density slice classification with the digitized vector overlay shows that aerial photograph to Landsat TM image registration error has not been insignificant in this study (Figure 7).

Figure 7 highlights two problems with the comparison of the classified TM data and the digitized ground-truth polygons. Clearly, when comparing high resolution ground-truth data with lower resolution test data, registration errors between the two datasets will be a problem. In this case the aerial photography was registered to the Landsat TM data until low RMS errors were achieved and a good visual fit was established. Even with this close checking of the registration, the best possible result is a registration error slightly less than the largest pixel size (30 m). This error can amount to a significant reported error in the classification, especially when the main features of interest are long, thin, and meandering.

The second feature highlighted by Figure 7 is the inclusion of sub-pixel sized polygons. These small polygons were included to determine whether Landsat TM data could be used to detect water bodies smaller than a pixel. Figure 7 shows a number of these features that are less than a pixel in width and even less than a pixel in total area. With these smaller features mis-registration severely reduced the possibility of an accurate result being reported, and the effect of mixed pixels further reduced the likelihood of an accurate classification.

Conclusion

From this study it is clear that Landsat TM data can be used to map water bodies associated with the Murrumbidgee River and its floodplain in the Wagga Wagga region. A multispectral maximum-likelihood classification was able to produce an overall classification accuracy of 97.4 percent. This classification was able to locate all of the major water bodies but underestimated the number of water pixels present on the image, achieving a producer's accuracy of only 59.6 percent.

Importantly, a simple density slice classification of the mid-infrared band 5 produced a classification accuracy (96.9 percent) similar to that of the maximum-likelihood classification. The density slice gave a better estimate of water pixels but tended to include more pixels that were not water bodies (user's accuracy 64.5 percent).

The other infrared bands, band 4 and band 7, were also useful for locating water bodies but tended to include more errors of commission. Lush crop areas were included in the band 7 density slice classification, and poor pasture, hill shadow, and parts of the urban area were included in the band 4 density slice classification.

All of the visible bands proved to be inadequate for successful density slice classification. The brightness of the turbid water showed a range of pixel values similar to that of the majority of the surrounding land cover, resulting in gross overestimation of the water area.

The infrared wavelengths are the most useful that optical scanners can offer for water mapping. The strong absorption of infrared light by water bodies gives them a distinctively low spectral response in this range. The mid-infrared bands of Landsat TM proved marginally more successful than the near-infrared band. The narrow nature of the water bodies in question creates many fringing mixed pixels that often contain significant responses from vegetation. Also, some of the water bodies

are very turbid, which increases the upper range of values in near-infrared more than it does in the mid-infrared bands. The combination of mixed pixels and high turbidity limits the use of a single near-infrared band to classify water bodies. This limitation has significant ramifications for the use of optical remotely sensed data such as those acquired by Landsat MSS or SPOT.

Acknowledgments

The authors thank Rodney Rumbachs for preparation of the aerial photography and the production of the location map and John Louis, David Roshier, David Lamb, and the anonymous reviewers from PE&RS for their comments on the manuscript.

References

Baumann, P., 1999. Flood Analysis, *http://www.research.umbc.edu/~tbenja1/baumann/mod2.html*, 10 February 1999.

Bennett, M.W.A., 1987. Rapid monitoring of wetland water status using density slicing, *Proceedings of the 4th Australasian Remote Sensing Conference*, [14–18 September], Adelaide, pp. 682–691.

Blackman, J.G., S.J. Gardiner, and M.G. Morgan, 1995. Framework for biogeographic inventory, assessment, planning and management of wetland systems: the Queensland approach, *Workshop Proceedings, Wetland Research in the Wet/Dry Tropics of Australia*, (C.M. Finlayson, editor), Jabiru, NT, Australia, Supervising Scientist Report No. 101, Department of Environment and Heritage, Canberra, pp. 114–122.

Brady, A., M. Shaikh, A. King, and P. Sharma, 1999. Remote sensing and the Great Cumbung Swamp, *Wetlands Australia*, 7:596–606.

Jensen, J.R., 1996. *Introductory Digital Image Processing: A Remote Sensing Perspective*. Prentice Hall, Upper Saddle River, New Jersey, 316 p.

Johnston, R., and M. Barson, 1993. Remote sensing of Australian wetlands: An evaluation of Landsat TM data for inventory and classification, *Australian Journal of Marine and Freshwater Research*, 44:235–252.

Kingsford, R.T., R.F. Thomas, P.S. Wong, and E. Knowles, 1997. *GIS Database for Wetlands of the Murray Darling Basin*, Final Report to the Murray-Darling Basin Commission, National Parks and Wildlife Service, Sydney, Australia, 85 p.

Lee, K.H., and R.S. Lunetta, 1995. Wetland detection methods, *Wetland and Environment Applications of GIS* (J.G. Lyon and J. McCarthy, editors), Lewis, Boca Raton, Florida, pp. 249–284.

Manavalan, P., P. Sathyanath, and G.L. Rajegowda, 1993. Digital image analysis techniques to estimate waterspread for capacity evaluations of reservoirs, *Photogrammetric Engineering & Remote Sensing*, 59(9):1389–1395.

Morse, A., T.J. Zarriello, and W.J. Kramber, 1990. Using remote sensing and GIS technology to help adjudicate Idaho water rights, *Photogrammetric Engineering & Remote Sensing*, 56(3):365–370.

Olive, L.J., J.M. Olley, Murray, and P.J Wallbrink, 1994. Spatial variation in suspended sediment transport in the Murrumbidgee River, New South Wales, Australia, *Variation in Stream Erosion and Sediment Transport*, (L.J. Olive, R.J. Loughran, and J.A. Kesby, editors), IAHS Publication 224, International Association of Hydrological Sciences, Canberra, pp. 241–249.

Olive, L.J. and J.M. Olley, 1997. River regulation and sediment transport in a semi-arid river: The Murrumbidgee River, New South Wales, Australia, *Proceedings of the Rabat Symposium, Human Impact on Erosion and Sedimentation*, April, Rabat, Morocco, pp. 283–290.

Overton, I., 1997. *Satellite Image Analysis of River Murray Floodplain Inundation*, NRMS Project R6045, Murray-Darling Basin Commission, Adelaide, 12 p.

Page, K.J., 1988. Bankfull discharge frequency for the Murrumbidgee River, New South Wales, *Fluvial Geomorphology of Australia* (R.F. Warner, editor), Academic Press, Sydney, pp. 267–281.

Phinn, S.R., L. Hess, and C.M. Finlayson, 1999. *An Assessment of Remote Sensing for Monitoring and Inventorying Wetland Environments in Australia*, report prepared for the National Wetlands Program, Environmental Research Institute of the Supervising Scientist, Environment Australia, Jabiru, Australia, 52, 45 p.

Pinneena, 1998. *New South Wales Surface Water Data Archive. Version 6*, Department of Land and Water Conservation, NSW, Australia (on a CD).

Shaikh, M., A. Brady, and P. Sharma, 1997. Applications of remote sensing to assess wetland inundation and vegetation response in relation to hydrology in the Great Cumbung Swamp, Lachlan Valley, NSW, Australia, *Wetlands for the Future* (A.J. McCumb and J.A. Davies, editors), Gleneagles Publishing, Glen Osmond, South Australia, pp. 595–606.

Smith, L.C., 1997. Satellite remote sensing of river inundation area, stage, and discharge: A review, *Hydrological Processes*, 11:1427–1439.

Thorley, N., S. Clandillon, and P. De Fraipont, 1997. The contribution of spaceborne SAR and optical data in monitoring flood events: Examples in northern and southern France, *Hydrological Processes*, 11:1409–1413.

(Received 26 March 1999; revised and accepted 09 November 1999)